



Adaptive solar building envelope with thermal energy storage

Chakraborti, S., Mondol, J. D., Smyth, M., Zacharopoulos, A., & Pugsley, A. (Accepted/In press). Adaptive solar building envelope with thermal energy storage. In *Unknown Host Publication* European Cooperation in Science and Technology. <http://www.tu1205-bists.eu/wp-content/uploads/sites/13/2017/03/Proceedings-of-BIRES-2017-01-01.pdf>

[Link to publication record in Ulster University Research Portal](#)

Published in:
Unknown Host Publication

Publication Status:
Accepted/In press: 05/03/2017

Document Version
Author Accepted version

General rights

Copyright for the publications made accessible via Ulster University's Research Portal is retained by the author(s) and / or other copyright owners and it is a condition of accessing these publications that users recognise and abide by the legal requirements associated with these rights.

Take down policy

The Research Portal is Ulster University's institutional repository that provides access to Ulster's research outputs. Every effort has been made to ensure that content in the Research Portal does not infringe any person's rights, or applicable UK laws. If you discover content in the Research Portal that you believe breaches copyright or violates any law, please contact pure-support@ulster.ac.uk.

Adaptive solar building envelope with thermal energy storage

Shauli Chakraborti^{*1}, Jayanta Deb Mondol¹, Mervyn Smyth¹, Aggelos Zacharopoulos¹, Adrian Pugsley¹

¹Centre for Sustainable Technologies, School of the Built Environment, Ulster University, Newtownabbey, Northern Ireland, BT37 0QB, UK

^{*}Corresponding author: S Chakraborti (E-mail: Chakraborti-S@email.ulster.ac.uk)

ABSTRACT

Conventional buildings are characterised by low and static heat transfer coefficients, which limit their thermal response to diurnal and seasonal meteorological changes. This leads to overall increased heating and cooling demand of the building to maintain the desired level of interior comfort. Appropriate thermal insulation strategies offer better thermal energy management and significant energy efficiency in buildings. An adaptive building shell, with flexible parameters (thermophysical/optical), that adjusts and utilises this variability to mediate indoor climates, could therefore logically address the problem.

Hence, this paper aims to demonstrate the potential of combining dynamic heat transfer mechanisms with thermal energy storage in a building wall prototype. The evacuation methodology proposed to vary the wall's thermal insulation is a novel way to efficiently control the heat transfer between the interior and exterior building environment. The dynamic insulation feature augments the heat storage capability of the wall, which could be utilised to provide space heating as and when required. Overall, the proposed wall prototype is expected to exploit the solar heat gain more effectively and have improved thermal response to transient environmental conditions.

To investigate the feasibility of this technology, the dynamic insulation feature needs to be realised as a part of initial experimental characterisation. A small scale test unit (representing one single component of the multi-component composite wall) was fabricated and its thermal performance was evaluated under steady simulated conditions.

Heat transfer through the tested component unit, under the different levels of evacuation was compared. Analysis of the experimental results indicates that the thermal transmittance through the tested component can be varied using this novel evacuation concept. Consequently, it can be concluded that this dynamic heat transfer technique offers the ability to affect and improve the thermal performance of a composite wall. Further, the study offers considerable scope to test the composite wall system with three components, predict generalised heat transfer correlations in evacuated enclosures and develop simulation models to validate and test its accuracy.

Key words: solar energy; building envelope; heat transfer; efficiency; thermal storage

1. INTRODUCTION

As energy demands continue to surge, so do the challenges; to address the hazards of climate change, incentivize energy efficiency, alleviate CO₂ emissions and secure sustainable green energy for the future. Energy efficiency is at the core of UK government's commitment, to reduction in overall CO₂ emissions by 80% by 2050. (Anon, 2016). A significant stimulus to the UK building industry has been provided by the dual demands of the Energy Performance of Buildings Directive (EPBD) "nearly zero" energy status for every new building and the active promotion of the Renewable Energy Services Directive (RES) to offset conventional fossil fuel use in buildings.(Aelenei et al.,2016).

The design of low energy buildings targets effective utilisation of renewable energy sources to meet energy demands and reduce energy consumption in buildings significantly through more energy efficient mechanisms. (Kalogirou, 2015). Several energy efficient technologies ranging from use of lightning, insulation, passive architecture, natural ventilation, phase change materials (PCM),intelligent controls, smart glazing, adaptive comfort, load shifting ,development of legislature, rating procedures and use of building integrated renewables have come to the fore in recent years. (Hu et al., 2016)

The building fabric and its novel optimised designs are drawing increasing attention in the solar energy research field. (Littlewood & Smallwood, 2015) The building fabric plays a significant role in regulating the thermal comfort of the indoor environment and reducing the overall heating and cooling demand of the building due to its ability to control the energy flow between the inner and outer space. Appropriate thermal insulation and good thermal energy storage are the core factors in improving the energy efficiency of buildings and are thus becoming more and more integral parts of the building component. An optimal building fabric design with enhanced static thermal insulation of the building envelope developed using PCM thermal storage is yet another approach to increase the energy efficiency.(Thirugnanasambandam et al., 2010) However, under variable indoor and/ outdoor meteorological conditions, it lacks control and consequentially affects the transient thermal behaviour of the building element(Omrany et al., 2016)

Extensive research in developing innovative, regenerative and sustainable energy efficient systems for buildings, is ongoing globally. However, most of these systems give rise to generic problems including high cost, installation hazards, bulky size, inefficient storage systems, inadequate energy efficiency ratios, undesirable temperature fluctuations and slower response to variable environmental parameters. (Shen et al., 2007; Sadineni et al., 2011; Saadatian et al,2012; Stazi et al., 2012;Hami et al., 2012)

This paper presents the potential for combining dynamic heat transfer mechanisms with thermal energy storage in a Dynamic Insulated Solar Building Envelope with Thermal Storage (DISBETS) concept. The DISBETS concept is fundamentally a passive solar thermal system targeted to collect, store and utilise solar radiations for space heating. However, this novel technology is designed to vary the overall thermal insulation of the building using a partial evacuation technique. It is expected that the DISBETS system will exploit the available solar heat gain more effectively than other solar wall systems and have overall improved thermal response to transient environmental conditions.

2. THE DISBETS TECHNOLOGY

The DISBETS technology consists of a composite system with three parallel chambers, designed to collect, store and utilise solar radiation for interior space heating. The integrated unit comprises of two identical square hollow vessels with an intermediate chamber between them which functions as a thermal store (see Fig.1). The hollow vessels are designed to regulate the direction of the flow of heat (depending on the heating/cooling demand of the building) via the evacuation technique. The outer face of the first hollow chamber, is blackened to act as the solar collector plate, absorbing part of the incident solar radiation. Thermal energy transmission from the absorber into the thermal storage occurs mainly by conduction through the chamber walls and convection of the air layer enclosed in the hollow chamber. The thermal storage not only helps to store the solar heat to be made available when required, it also ensures improved interior thermal comfort by alleviating thermal fluctuations. The innermost hollow chamber is either partially evacuated or maintained at atmospheric pressure depending on the heating demand of the building. The DISBETS system is designed to perform optimally under three different conditions as follows:

- 1) During periods of solar abundance, the outer hollow chamber, maintained at atmospheric pressure, absorbs the incident solar radiations and transfers it into the thermal storage. The inner hollow chamber, is partially evacuated to prevent heat transfer from the storage into the building interior to prevent overheating.
- 2) During non collection periods (eg. night time and cloudy periods), the first chamber is evacuated to lower pressure, to minimise heat loss from thermal storage into the building exterior. The thermal energy, thus remains preserved in the thermal storage, to be released later for interior space heating.
- 3) When this stored heat is required, the inner hollow chamber, hereto evacuated to lower pressure is allowed to fill with air at atmospheric pressure. This helps facilitate heat transfer from the thermal storage into the interior by convection of the air layer inside the chamber.

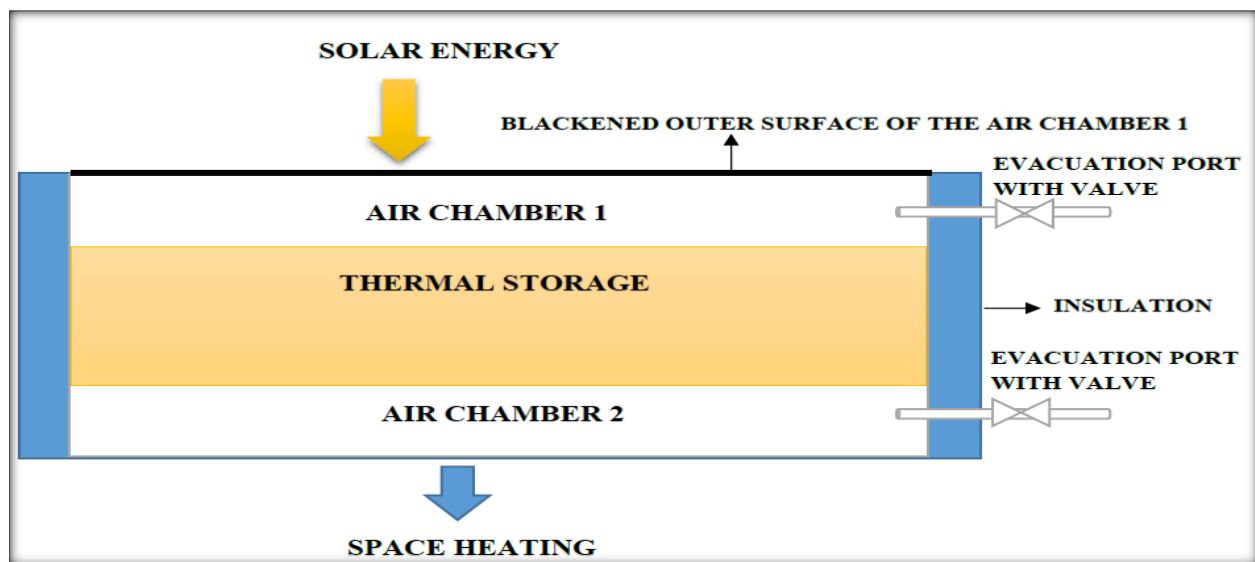


Fig.1 Schematic of the DISBETS concept

3. FABRICATION OF THE DISBETS PROTOTYPE COMPONENTS

A small scale prototype of the DISBETS's first two chambers (a hollow chamber and a thermal store) was designed and fabricated to investigate its thermal performance under simulated conditions. The outer hollow chamber consisted of a base tray and a cover tray both fabricated using 304 L stainless steel of 0.85mm thickness. The base tray 510mm \times 510mm \times 45mm, was supported by an internal framework of six stainless steel ribs. A stainless steel tube of outer diameter 6mm was welded to the base tray to function as the evacuation port. (See Fig.2a). The front surface of the base tray was uniformly sprayed with matt black stove paint (radiative absorptance ~ 0.9) to augment solar absorption. The supporting skeleton of the structural ribs is necessary to ensure the structural stability of the hollow chamber under partial evacuation and prevent it from collapsing under the influence of the atmospheric pressure acting on the external surfaces. Each individual supporting rib was a simple stainless steel 445 mm long angle section 18mm \times 18mm \times 0.9mm. The framework consisted of three parallel stainless steel ribs spot welded to the base of the tray, separated by a distance of 125mm from each other. The remaining three ribs, were positioned parallel to each other and perpendicular to the base ribs. Each individual rib was again distanced by 125mm from each other and spot welded to the base ribs, to form a regular grid.

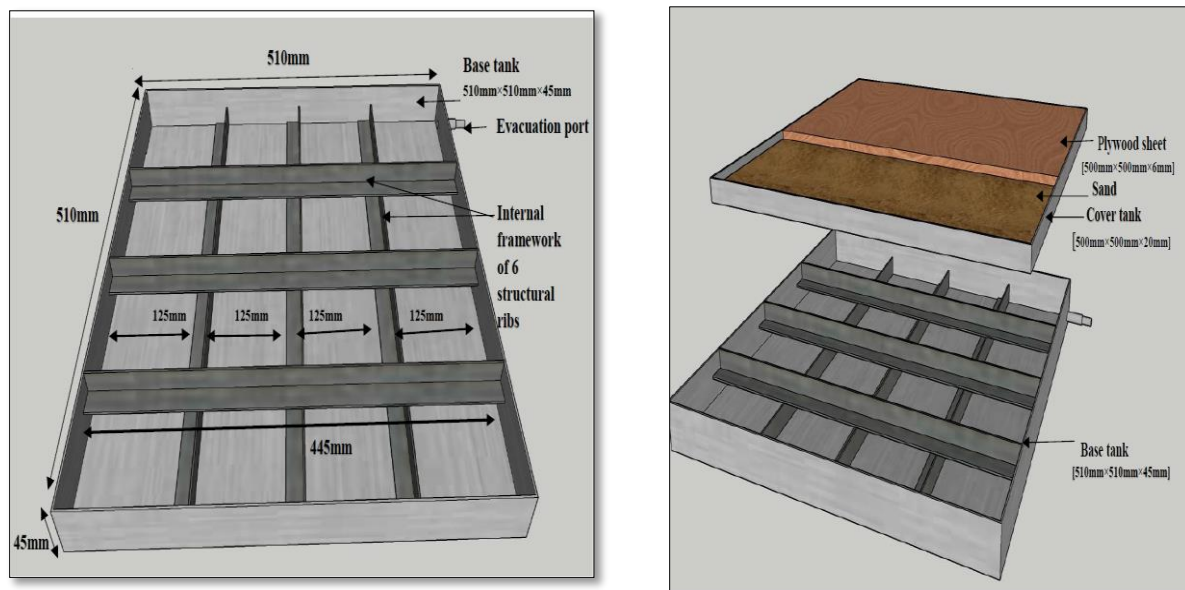


Fig.2 a) Base tray with structural ribs b) Schematic of the fabricated hollow chamber with thermal mass

The cover tray 500mm \times 500mm \times 20mm was also fabricated of stainless steel. The cover tray sits inside the base tray. The cover tray was welded to the base tray with its base sitting on the ribbed grid of the deeper base tray creating a 25mm cavity between the two walls of the outer hollow chamber. The 20 mm deep cavity of the cover tray was used to contain the thermal mass. Seven kilograms of common fine grain builder's sand was used as thermal storage. The sand is thoroughly dried, sieved and carefully measured out into the storage cavity. The thermal storage was enclosed within the 20 mm cavity and a 500mm \times 500mm \times 6mm plywood sheet securely taped all around

to hold it in place.(See Fig.2b).The fabricated two chambered DISBETS prototype component was well insulated on all the sides with 50 mm polystyrene foam insulation to minimise thermal losses.(See Fig.3a and 3b).

4. EXPERIMENTAL SET UP AND METHODOLOGY

Short term investigative studies on the thermal performance of the two chambered DISBESTS prototype component was conducted under the indoor solar simulator facility at the Ulster University. The schematic of the experimental set up is shown in Fig.3a. The simulator lamp array consists of 35 high power halide lamps arranged in 7 rows of 5 lamps each. (Zacharopoulos et al., (2009) The solar simulator dimming control panel was used to adjust and set a sustained illumination on the test area surface. A high precision, high temperature CM4 pyranometer (Kipp & Zonen) was used to monitor the simulated irradiance by placing it on several positions on the test unit surface. Fig. 3b) shows the frontal view of the component tested unit mounted on a wooden frame and positioned vertically to face the simulated radiation on-axis.

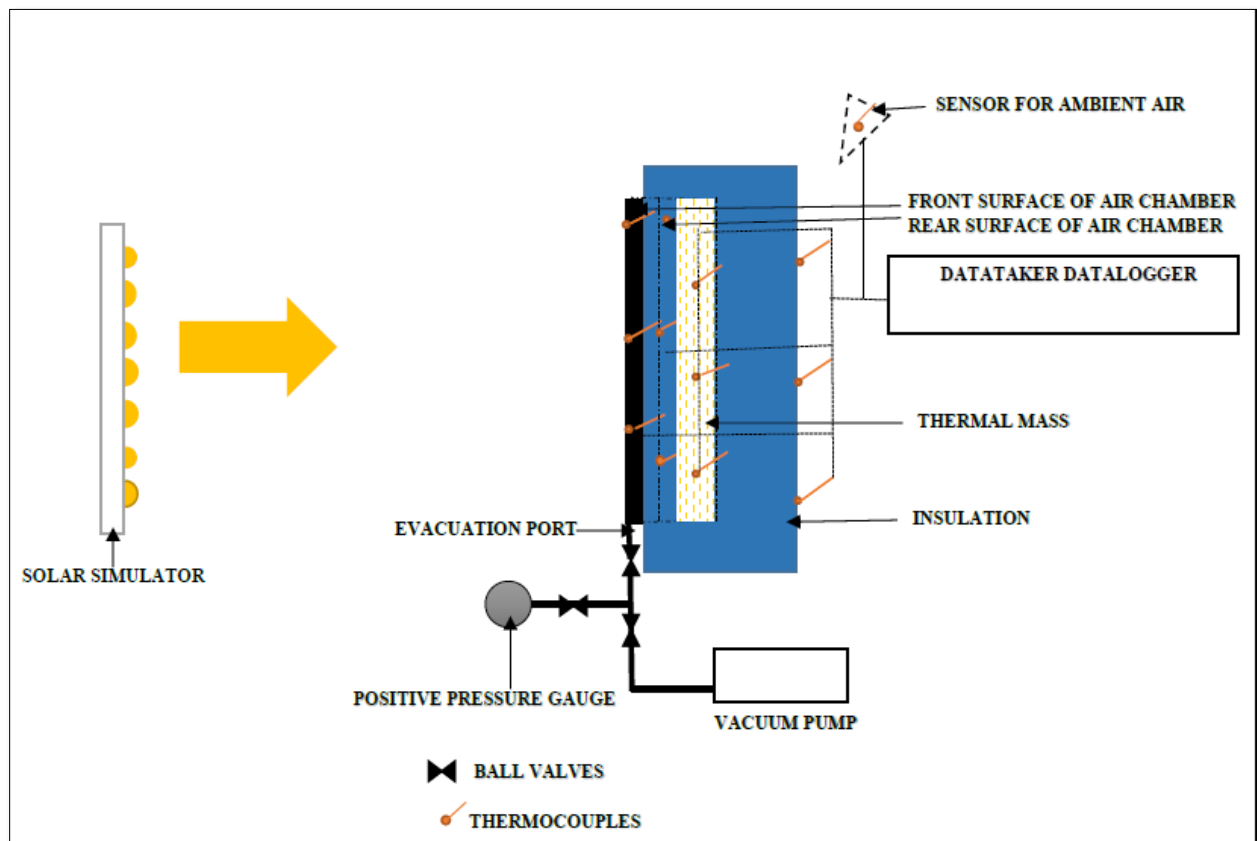


Fig.3a) Schematic view of the experimental set-up

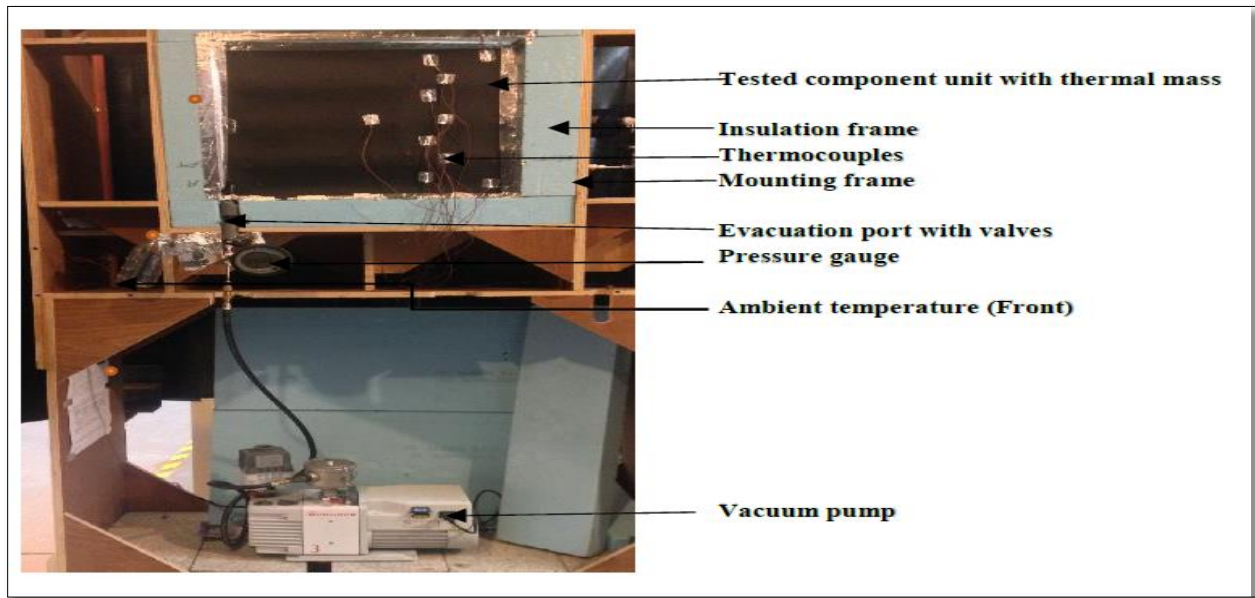


Fig.3 b) DISBETS component test rig ready for indoor testing under the solar simulator facility

T-type copper constantan thermocouples with estimated temperature measurement uncertainty of $\pm 0.5^\circ \text{C}$, were used to monitor and record the temperatures of the various surfaces of the hollow air chamber, thermal storage and ambient air. Data measurements from sensors were logged and transferred to the computer using a stand alone Data Taker datalogger unit. The hollow air chamber was partially evacuated using a two-stage rotary vane oil sealed vacuum pump connected to the chamber via the ball vacuum valve on the evacuation port. The pressure levels were monitored using a digital positive pressure gauge. Prior to the start of experiment, the test chamber, with all the vacuum fittings was tested for leakage and structural stability under evacuated conditions. Once the solar simulator was switched on, it was allowed to warm up for around 30 minutes in order to stabilise the fluctuations in irradiance. During this period the test area was shielded from the simulator. The intensity of radiation was measured by placing the pyranometer on five premarked positions. The effective irradiance was calculated by averaging these measured values. The main test was subsequently initiated by removing the shading, and data logging was activated. All tests were conducted under a simulated irradiance of 774 W/m^2 . Each test lasting for 6 hours was split into 3 hours of collection followed by 3 hours of cooling period. The unit was left to normalise overnight to return to the ambient conditions before subsequent tests were undertaken. To investigate the effectiveness of the lower pressure levels in providing improved thermal insulation and minimising thermal losses, the unit was tested under two different pressure scenarios. In the first test the hollow air chamber was partially evacuated to 2 mbar over the entire test period, whereas in the second test the pressure level in the chamber was maintained nearer to atmospheric pressure (758mbar).

5. EXPERIMENTAL RESULTS AND ANALYSIS

The overall front and the back surface temperatures of the chamber were calculated by averaging the values of the strategically positioned temperature sensors. The measured average front (T_F) and back surface (T_B) temperature time histories over the entire six hour period of each test is

represented graphically in Fig.4a) and Fig 4b) respectively. The results show that the front (T_F) and the back surface (T_B) temperatures of the tested air chamber with higher pressure level (758 mbar), rose to 67.0 °C and 54.2 °C, respectively over a period of 3 hours of continuous irradiance . The corresponding front and back surface temperatures of the same unit with a lower internal pressure level (2 mbar), were 68.4 °C and 52.1 °C, respectively. Table 1 summarises the front and back surface temperature measurements over a test period of the first 3 hours for both pressure levels.

Table 1. Temperatures achieved by the front and back surface of the DISBETS test component chamber after first 3 hours for 758mbar and 2 mbar pressure levels

Intensity of illumination	Air Pressure inside the test chamber	Ambient air temperature	Front surface temperature	Back surface temperature	Temperature Difference between the front and back surface ($\Delta T_{\text{Chamber}}$) = $T_F - T_B$
[W/m ²]	[mbar]	[°C]	[°C]	[°C]	[°C]
774	758	29.2	67.0	54.2	12.7
774	2	29.0	68.4	52.1	16.3

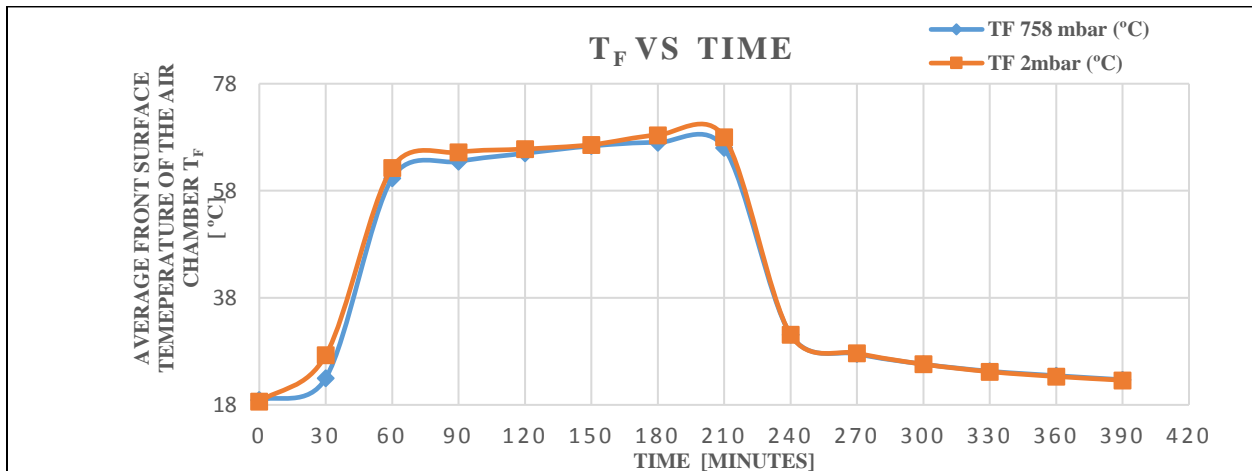


Fig. 4 a) Front surface temperature (T_F) time histories for two different chamber pressure levels profile for both pressure levels over the entire test period

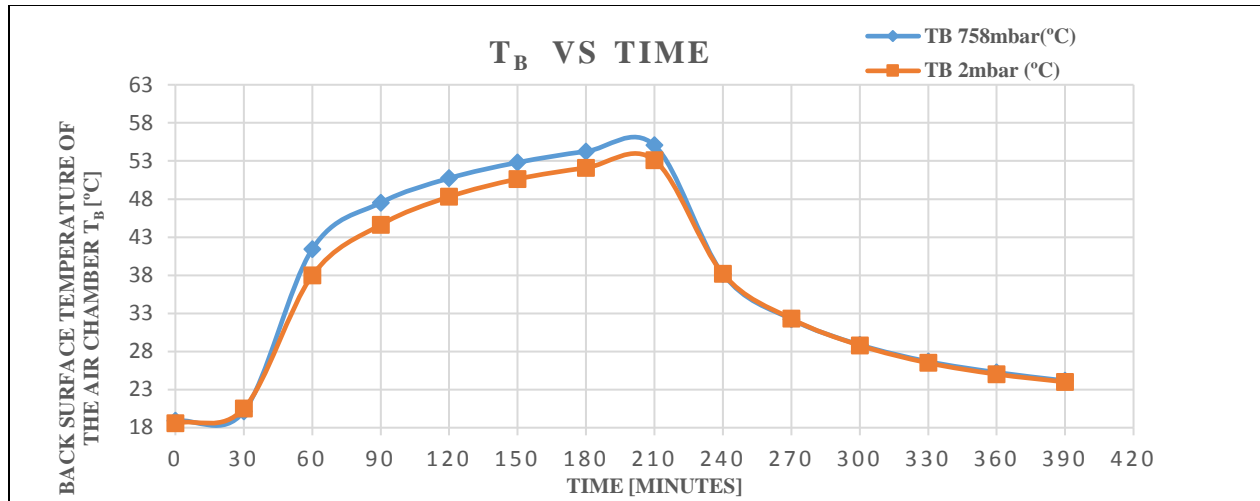


Fig. 4 b) Back surface temperature (T_B) temperature time histories for two different chamber pressure levels profile for both pressure levels over the entire test period.

The measured temperature difference ($\Delta T_{\text{Chamber}}$) between the front and back surface of the tested air chamber for the two pressure levels (758 mbar and 2 mbar) over the entire test period is shown in Fig. 5.

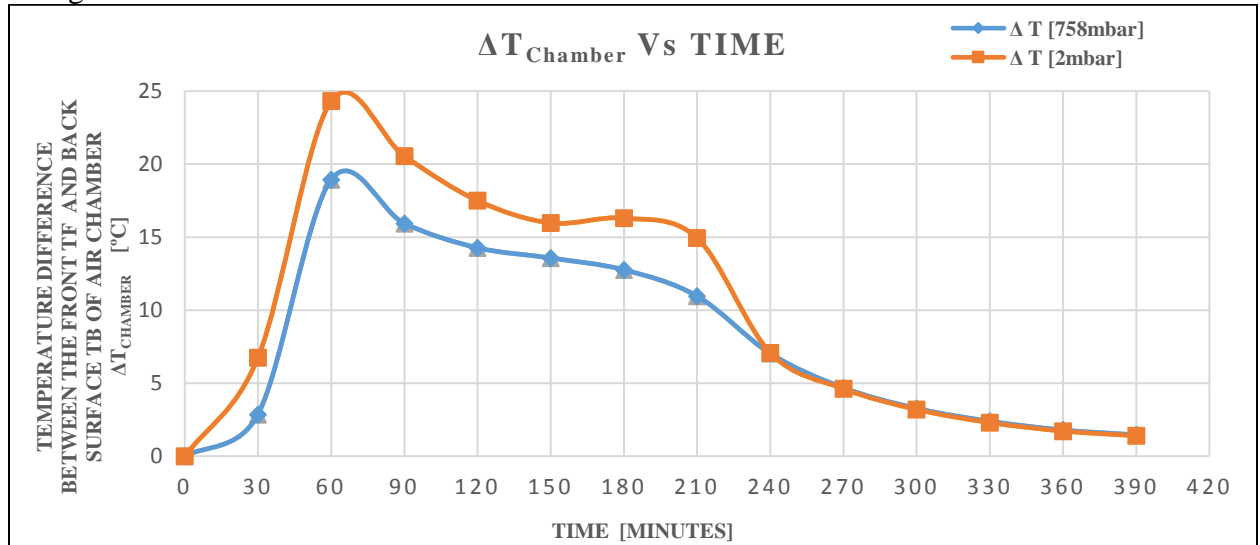


Fig 5. Temperature difference time history for two different chamber pressure levels profile for both pressure levels over the entire test period.

As expected, the temperature difference ($\Delta T_{\text{Chamber}}$) was 3.6 °C higher in the lower pressure (2mbar) than in the near-atmospheric pressure (758mbar) level. This is because for pressure level of 2mbar, there is less convective heat transfer than for the 758mbar pressure level, due to the reduced mass of gas (air) inside the hollow chamber. Hence, the front surface temperature was higher by 1.4 °C, and the back surface temperature was lower by 2.1 °C in case of 2mbar pressure compared to 758mbar pressure level. The temperature of the thermal mass ($T_{\text{thermalmass}}$) over each energy collection test period, was measured. The rise in temperature of the thermal mass was 30.0 °C in 3 hours when the chamber pressure was 758mbar, while the corresponding rise in temperature, in 3 hours for lower chamber pressure of 2mbar was recorded to be 28.6 °C. The

initial and final temperature of the thermal mass during the hours of collection are presented in Table 2. A higher front surface temperature for lower pressure [2mbar], indicates lower heat transfer into the chamber and subsequently into the thermal mass. This is validated by the lower temperature of the thermal mass, when the chamber air pressure is lower. The higher thermal mass temperature for higher pressure level [758mbar] indicates greater heat transfer compared to the lower pressure level inside the air chamber.

Table 2. Initial and final temperatures of the thermal mass as recorded at the start and end three hour test for 758mbar and 2mbar pressure levels.

Intensity of illumination	Air Pressure inside the test chamber	Ambient air temperature	Initial temperature of thermal mass	Final temperature of thermal mass	Temperature Difference between final and initial temperature of thermal mass ($\Delta T_{\text{thermalmass}}$) = $T_{t=3\text{hrs}} - T_{t=0}$
[W/m ²]	[mbar]	[°C]	[°C]	[°C]	[°C]
774	758	29.2	18.5	48.5	30.0
774	2	29.0	18.4	47.0	28.6

Temperature difference between the initial and final temperatures of the thermal mass ($\Delta T_{\text{thermalmass}}$) over a test period of three hours is calculated using equation (1). Heat transfer through the tested air chamber is quantified by the amount of heat accumulated by the thermal mass over the test period (first 3 hours). The heat energy collected (Q_c) by the thermal mass, instantaneous thermal power gained (q_c) and the corresponding thermal conductance (U_c) are calculated using the equations (2), (3) and (4) respectively.

$$\Delta T_{\text{thermalmass}} = T_{t=i} - T_{t=f} \quad (1)$$

$$Q_c = m c_p \Delta T_{\text{thermalmass}} \quad (2)$$

$$q_c = \frac{Q_c}{\Delta t} \quad (3)$$

$$U_c = \frac{q_c}{A(T_F - T_B)} \quad (4)$$

The amount of heat energy collected was calculated using Eq. (2). For the higher (758mbar) pressure level inside the test chamber, cumulative heat collected over the entire three hour collection period of three was 161.8 kJ, while for the lower pressure (2mbar), it was calculated to be 156.8kJ. Hence, heat gained is reduced by 5kJ, when the chamber is evacuated to lower (2mbar) pressure level. The thermal transmittance calculated using Eq. (4) was found to rise steadily faster

in case when the chamber was at higher pressure. The thermal transmittance values of the tested chamber, at the end of the first three hour test period, for the highest recorded thermal storage temperatures were compared to analyse the effectiveness of changing the pressure level to regulate the heat transfer. At the higher pressure level of 758mbar inside the tested chamber the thermal conductance value derived for the last 30 minutes of the collection period ($t=150$ minutes to $t=180$ minutes) was $6.63 \text{ W/m}^2 \text{ K}$, while, the corresponding value at the lower pressure level of 2mbar was $4.6 \text{ W/m}^2 \text{ K}$.

6. CONCLUSIONS

The experimental evaluation of the small scale DISBETS component test unit comprising only of a part of the entire composite wall system indicates that the test unit is performing as expected. The structural stability of the air chamber component of the DISBETS composite system is very crucial as the chamber is to be evacuated to different pressure levels. This design of the chamber is found to be structurally stable and seems to work intuitively under different levels of evacuation. Heat transfer through the tested component unit was examined, for two different levels of evacuation of the hollow chamber. When the hollow chamber was evacuated to a lower pressure (2mbar), the total heat energy transferred through it into the thermal mass was lower than when the chamber was evacuated to only marginally below atmospheric pressure (758mbar). The front to back surface temperature difference was consistently higher when evacuated to 2 mbar than at the higher internal chamber pressure of 758mbar. This indicates lower thermal transmittance through the chamber and consequently lower heat gain into the thermal store when the hollow chamber is evacuated. Though the heat gain into the thermal store for higher internal pressure (758mbar) of the hollow chamber is not significantly higher (being only 5kJ greater), than when the hollow chamber is evacuated to lower pressure level of 2mbar; it is still deemed acceptable that changing the internal pressure level of the hollow chamber, thermal transmittance through the chamber and consequently heat gain into the thermal store can be affected by the proposed evacuation methodology. The observed performances points out the importance of lower pressure levels in the air chamber. A higher heat gain is anticipated with lower thermal losses from the exposed blackened surface of the test unit. Adding a transparent cover to the front surface of the unit will help minimise radiative and convective thermal losses and increase the amount of heat gained by the thermal store.

The study shows that the proposed hollow chamber evacuation concept affects the heat transfer into the thermal storage. Consequently, this offers considerable potential for the effectiveness of the integrated DISBETS system with two air chambers combined with thermal storage, to exploit solar gain more effectively. It is expected that the composite system with its unique dynamic heat transfer mechanism will have an overall improved thermal response to the transient environmental conditions.

NOMENCLATURE

ΔT	temperature difference ($^{\circ} \text{C}$)
T	temperature ($^{\circ} \text{C}$)
Q_c	thermal heat collected during the first three hours (kJ)
q_c	instantaneous thermal power gained during the first three hours (W)
m	mass of thermal storage (kg)

c_p	specific heat capacity of thermal storage material (J/kg K)
t	time since the start of the test
t=i	time at the start of observation period
t=f	time at the end of observation period
Δt	duration of test period (s)
A	area of the test chamber exposed to simulations (m ²)
U_c	thermal conductance during the first three hours (W/ m ² K)

SUBSCRIPT

Chamber	air chamber of the DISBETS component test unit
F	front surface temperature of the test chamber
B	back surface temperature of the test chamber
Amb	ambient air
thermalmass	thermal mass (dry builder's sand)

REFERENCES

Anon. *Meeting Carbon Budgets - 2016 Progress Report to Parliament Committee on Climate Change Presented to Parliament pursuant to Section 36(1) of the Climate Change Act 2008.* June 2016. <https://www.theccc.org.uk/publications/>.

Aelenei, L., Smyth, M., Platzer, W., Norton, B., Kennedy, D., Kalogirou, S. and Maurer, C. (2016) Solar Thermal Systems – Towards a Systematic Characterization of Building Integration. *Energy Procedia*, 91 897-906.

Hami, K., Draoui, B. and Hami, O. (2012) The thermal performances of a solar wall. *Energy*, 39 (1), 11-16.

Hu, Z., He, W., Ji, J. and Zhang, S. (2016) A review on the application of Trombe wall system in buildings. *Renewable and Sustainable Energy Reviews*, <http://dx.doi.org/10.1016/j.rser.2016.12.003>

Kalogirou, S.A. (2015) Building integration of solar renewable energy systems towards zero or nearly zero energy buildings. *International Journal of Low-Carbon Technologies*, 10 (4), 379-379.

Littlewood, J.R. and Smallwood, I. (2015) Testing Building Fabric Performance and the Impacts Upon Occupant Safety, Energy Use and Carbon Inefficiencies in Dwellings. *Energy Procedia*, 83 454-463.

Omran, H., Ghaffarianhoseini, A., Ghaffarianhoseini, A., Raahemifar, K. and Tookey, J. (2016) Application of passive wall systems for improving the energy efficiency in buildings: A comprehensive review. *Renewable and Sustainable Energy Reviews*, 62 1252-1269.

Saadatian, O., Sopian, K., Lim, C.H., Asim, N. and Sulaiman, M.Y. (2012) Trombe walls: A review of opportunities and challenges in research and development. *Renewable and Sustainable Energy Reviews*, 16 (8), 6340-6351.

Sadineni, S.B., Madala, S. and Boehm, R.F. (2011) Passive building energy savings: A review of building envelope components. *Renewable and Sustainable Energy Reviews*, 15 (8), 3617-3631.

Shen, J., Lassue, S., Zalewski, L. and Huang, D. (2007) Numerical study on thermal behavior of classical or composite Trombe solar walls. *Energy and Buildings*, 39 (8), 962-974.

Stazi, F., Mastrucci, A. and Munafò, P. (2012) Life cycle assessment approach for the optimization of sustainable building envelopes: An application on solar wall systems. *Building and Environment*, 58 278-288.

Thirugnanasambandam, M., Iniyar, S. and Goic, R. (2010) A review of solar thermal technologies. *Renewable and Sustainable Energy Reviews*, 14 (1), 312-322.

Zacharopoulos, Aggelos, Mondol, Jayanta Deb, Smyth, Mervyn, Hyde, Trevor and O'Brien, Vincent (2009) *State of the art solar simulator with flexible mounting*. In: ISES Solar World Congress, Johannesburg, South Africa. International Solar Energy Society. 10 pp.